Geological Society, London, Special Publications

# Crack-seal patterns: records of uncorrelated stress release variations in crustal rocks

François Renard, Muriel Andréani, Anne-Marie Boullier and Pierre Labaume

*Geological Society, London, Special Publications* 2005; v. 243; p. 67-79
doi:10.1144/GSL.SP.2005.243.01.07

# Crack–seal patterns: records of uncorrelated stress release variations in crustal rocks

FRANÇOIS RENARD[1,2], MURIEL ANDRÉANI[1], ANNE-MARIE BOULLIER[1] & PIERRE LABAUME[3]

[1]*LGIT, Université Joseph Fourier, BP 53, 38041 Grenoble, France (e-mail: francois.renard@lgit.obs.ujf-grenoble.fr)*

[2]*Physics of Geological Processes, Institute of Physics, postboks 1048 Blindern, 0316 Oslo, Norway*

[3]*Dynamique de la lithosphère (UMR5573), Université Montpellier II, place E. Bataillon, 34095 Montpellier Cedex 5, France*

**Abstract:** Statistical properties of crack–seal veins are investigated with a view to assessing stress release fluctuations in crustal rocks. Crack–seal patterns correspond to sets of successive parallel fractures that are assumed to have propagated by a subcritical crack mechanism in the presence of a reactive fluid. They represent a time-sequence record of an aseismic and anelastic process of rock deformation. The statistical characteristics of several crack–seal patterns containing several hundreds of successive cracks have been studied. Samples were collected in three different areas, gold-bearing quartz veins from Abitibi in Canada, serpentine veins from the San Andreas system in California and calcite veins from the Apennine Mountains in Italy. Digitized pictures acquired from thin sections allow accurate measurement of crack–seal growth increments. All the samples show the same statistical behaviour regardless of their geological origin. The crack–seal statistical properties are described by an exponential distribution with a characteristic length scale and do not show any spatial correlation. They differ from other fracture patterns, such as earthquake data, which exhibit power-law correlations (Gutenberg–Richter relationship). Crack–seal series represent a natural fossil record of stress release variations (less than 50 bars) in the crust that show a characteristic length scale, associated with the resistance of rock to effective tension, and no correlation in time.

## Introduction

Syntectonic calcite or quartz veins with a crack–seal structure are common in rocks at low metamorphic grades and high fluid pressure (Beach 1977; Ramsay & Huber 1983; Passchier & Trouw 1995). The formation of these veins can be explained by a growth mechanism involving many repeated small increments, the crack–seal process (Ramsay 1980). The overall pattern is the result of a sequence of crack increments, followed by periods of precipitation in the open cracks (Fig. 1). Veins attributed to the crack–seal mechanism are commonly considered as evidence of episodic crack opening, driven by oscillations in fluid pressure or bulk stress (Ramsay 1980; Cox 1991; Fisher & Brantley 1992; Petit *et al.* 1999). It is common to observe several hundred successive crack–seals, which therefore represent a fossil record of local elastic stress releases in the crust. However, to the authors' knowledge, no quantitative studies have been conducted on the level of stress variations and their correlations in time. Other fracturing processes in the crust exhibit well-defined correlations, the most famous being the power-law correlations widely found in large sets of fractures (Bonnet *et al.* 2001).

Indicators of crack–seal processes are regularly spaced bands of small inclusions (typically small minerals, pieces of wall rock, or fluid inclusions), aligned parallel to the vein walls. Inclusion trails at high angles to the walls are better indicators of the opening direction than fibrous crystals. Opening per crack event is generally in the order of several micrometres to several tens of micrometres (Cox & Etheridge 1983; Cox 1987; Williams & Urai 1989; Xu 1997).

The cracking event corresponds to the opening of a narrow fluid-filled crack along the vein

*From*: GAPAIS, D., BRUN, J. P. & COBBOLD, P. R. (eds) 2005. *Deformation Mechanisms, Rheology and Tectonics: from Minerals to the Lithosphere*. Geological Society, London, Special Publications, **243**, 67–79.
0305-8719/05/$15.00 

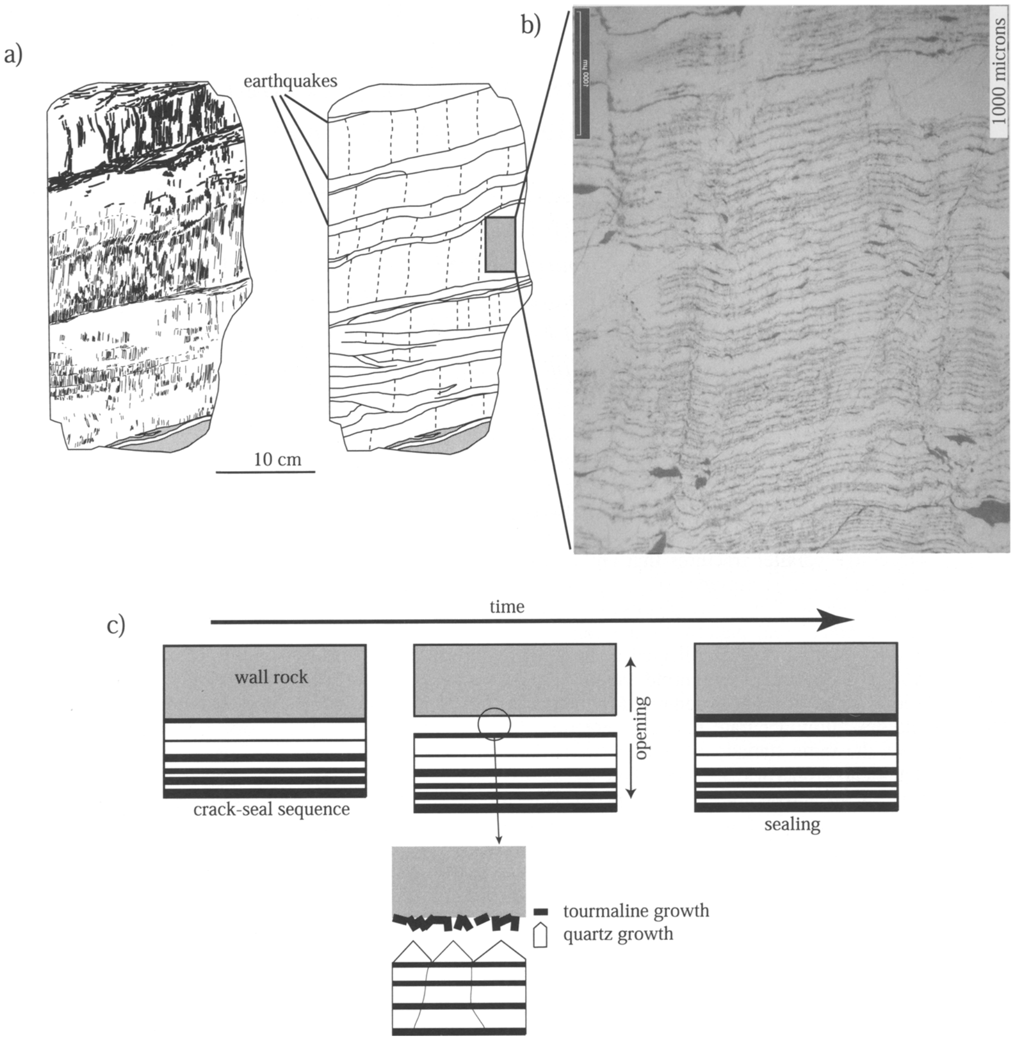


**Fig. 1.** (**a**) Sketch of a polished section of fibrous gold-bearing quartz vein, Abitibi, Canada, showing decimetre-scale organization of fibrous ribbons, separated by horizontal discontinuities, due to earthquake events (after Firdaous, 1995). Crack–seal patterns analysed in this study are located in the grey area. (**b**) Microscopic view of crack–seal structure. Quartz layers (light) alternate with tourmaline (dark). Pattern results from cracking events, followed by precipitation of minerals at the walls of open crack. (**c**) Diagram of crack–seal process. One tourmaline layer (dark) and one quartz layer (light) result in a cracking event, followed by precipitation.

margin, whereas, during the sealing period, precipitates fill the crack again (van der Pluijm 1984; Beutner & Diegel 1985; Ellis 1986; Gaviglio 1986; Cox 1987; Ramsay & Huber 1983; Labaume *et al.* 1991; Davison 1995; Fisher *et al.* 1995; Toriumi & Hara 1995). The precipitating crystals usually have a fibrous, elongate or blocky shape (Bons 2000).

Urai *et al.* (1991) proposed a kinematic numerical model for the formation of fibrous morphologies by a crack–seal mechanism, and predicted that, depending on the boundary conditions, fibres may or may not track the opening trajectory of the crack. In such a kinematic model, the displacement-tracking conditions in crack–seal veins are of two kinds. First, the vein wall should have a rough morphology and, secondly, the growth rate of fibres should be sufficiently fast to fill the open space before the next cracking event (Urai *et al.* 1991; Hilgers 2000).

Computer models of crack–seal fibrous veins have focused on studying the kinematics of vein-precipitation by varying different parameters, such as mineral morphology (e.g. prismatic growth), crack width, roughness, opening frequency and opening trajectory (Hilgers 2000).

The nutrients filling the vein can be transported by diffusion from the wall rock or by advection into the flow through the fracture network (Taber 1916, 1918; Boullier & Robert 1992; Fisher & Brantley 1992; Bons & Jessell 1997). Precipitation in the vein can be due to variations in fluid pressure (e.g. associated with fracturing) or to some nucleation process where new crystals can only grow on the fracture walls. Wiltschko & Morse (2001) proposed that cracking events could be due to the force of crystallization of the growing crystals, inducing subcritical crack propagation through stress concentration at the crack tip.

The crack–seal mechanism has been invoked to sustain the concept of fluid valving, an idea derived from considerations of fluid behaviour within and surrounding faults and shear zones, particularly associated with the seismic cycle (Sibson *et al.* 1988). As crack–seal structures record a time sequence of geological events, they represent a unique natural record of episodic events of cracking, whereby time periods are directly imprinted in the rock.

In this contribution, the statistical properties of crack–seal patterns in various rocks are studied and are related to stress release variations and their correlations in time. The aim is to characterize the apparent regularity of crack–seal increments and their spatial correlation. This provides new constraints on local states of stress in the crust in various geological settings.

## Geological setting and description of the crack–seal samples

Three kinds of crack–seal samples were collected and analysed (see Table 1): three quartz veins in diorite from Abitibi, Canada, two serpentine veins from California, and one calcite vein from the Apennines, Italy. It is shown below that, even if they come from various geological areas, these three kinds of samples have similar statistical distributions and spatial correlation properties.

### *Gold quartz-bearing veins, Val d'Or, Abitibi, Canada*

The structural setting of the gold-quartz veins at Val d'Or (Abitibi) has been described by Robert (1990) and Robert *et al.* (1995). The Val d'Or district is located in the Archean Abitibi greenstone belt, in which several shear zones of different scales were active during the late stages of a N–S shortening event and contain the quartz-tourmaline-carbonate-pyrite (QTC) veins considered in this paper (Robert 1990; Robert *et al.* 1995). The QTC vein system at the Sigma deposit occurs in deformed andesites, porphyritic diorites, and feldspar porphyry dikes

**Table 1.** *Top, origin and mineralogy of crack–seal veins. Middle, statistical properties of crack–seal samples: number of crack–seal events in the sample, thickness of vein, mean and standard deviation of thickness of individual crack–seal events in each vein, minimal thickness of individual cracks. Bottom, stress release variations recorded by crack–seals, assuming elastic properties.*

| Reference sample | S42abc | S42cdeg | S42lhijm | SY3P | SY32 | X45FXC |
|---|---|---|---|---|---|---|
| Location | Abitibi | Abitibi | Abitibi | Santa Ynez | Santa Ynez | Apennines |
| Country | Canada | Canada | Canada | CA, USA | CA, USA | Italy |
| Wall rock | Diorite | Diorite | Diorite | Serpentinized | Peridotite | Limestone |
| Vein filling minerals | Quartz + Tourmaline | | | Chrysotile | | Calcite |
| No. of successive cracks | 229 | 436 | 1106 | 88 | 251 | 379 |
| Vein thickness (μm) | 10100 | 16300 | 31900 | 350 | 570 | 56372 |
| Mean crack thickness (μm) | 44.4 | 37.6 | 28.9 | 4.1 | 2.3 | 148.7 |
| Std. crack thickness (μm) | 48.7 | 35.5 | 30.8 | 2.1 | 0.8 | 86.9 |
| Min. crack thickness (μm) | 12.0 | 8.1 | 7.2 | 1.3 | 0.8 | 21.8 |
| $E$ (kbar)[a] | 500 | 500 | 500 | 300 | 300 | 150 |
| $w$ ($\times 10^{-6}$ m)[b] | 44 | 38 | 29 | 4 | 2 | 149 |
| $c$ (m)[c] | 0.5–3 | 0.5–3 | 0.5–3 | 0.02 | 0.02 | 0.1 |
| $wE/4c$ (bar) | 11–66 | 10–60 | 7–42 | 15 | 7.5 | 56 |

[a]Wall-rock Young's modulus.
[b]Average crack thickness (see Fig. 5).
[c]Crack length data represent maximum values of the actual crack lengths.

(Robert & Brown 1986). The Sigma deposit combines subvertical shear zone-hosted fault veins and subhorizontal extensional veins, which display mutually cross-cutting relationships, cyclic growth and deformation textures and earthquake evidence (Boullier & Robert 1992). A seismic fault-valve model, involving fluctuations in fluid pressure, has been proposed to explain such cyclic sequences (Sibson *et al.* 1988).

The crack–seal vein studied here is a 60 cm thick subhorizontal tabular extensional vein, extending into intact rocks away from the associated fault veins in the Sigma deposit (Fig. 1a). It consists of several centimetre-scale wall-parallel ribbons of quartz and tourmaline representing growth layers and attesting to incremental development during successive earthquakes. These ribbons are themselves made of numerous crack–seal increments ranging between 7 and 200 $\mu$m in thickness (Figs 1b and 2). The opening direction was vertical, which implies a fluid pressure slightly higher than the lithostatic load during the formation of the vein (Boullier & Robert 1992). Quartz infilling has an elongate blocky structure in which crystals have a vertical long axis. The width of the crystals is 1 $\mu$m on average. Delicate undeformed tourmaline needles grow in rosettes on the inclusion bands on both sides of a crack–seal increment. We infer that they have crystallized in fluid-filled open-space cavities (Fig. 2b). The crack–seal structure is comparable to that described by Henderson *et al.* (1990); that is, inclusion bands are locally interrupted. Such interruptions of the crack–seal sequence also occur at a smaller scale of a few bands within the quartz crystals (Figs 1 and 2a). However, crack–seal sequences remain identical on both sides of the interruption, regardless of its scale, and may be followed over the entire width of large thin sections (7 cm) and from one sample to another.

The delicate geometry of crack–seal inclusion bands and the presence of undeformed tiny tourmaline fibres, that are not broken, indicate that the crack propagated slowly. Robert & Boullier (1994) have proposed that these crack–seal textures are induced by a steady-state mechanism of subcritical crack propagation in order to explain their constant shape mimicking the irregularities of the crack walls. The cracks followed the weak boundary between the host rock and the previous sealed crack. Like other authors (Robert & Boullier 1994; Cox 1995; Wiltshko & Morse 2001), we infer that crack propagation occurred in subcritical conditions. Based on experimental work, crack velocity may be estimated in the range $10^{-6}$ to $10^{-3}$ m s$^{-1}$, depending on stress, temperature, and fluid composition (Atkinson 1984; Guéguen & Palciauskas 1994).

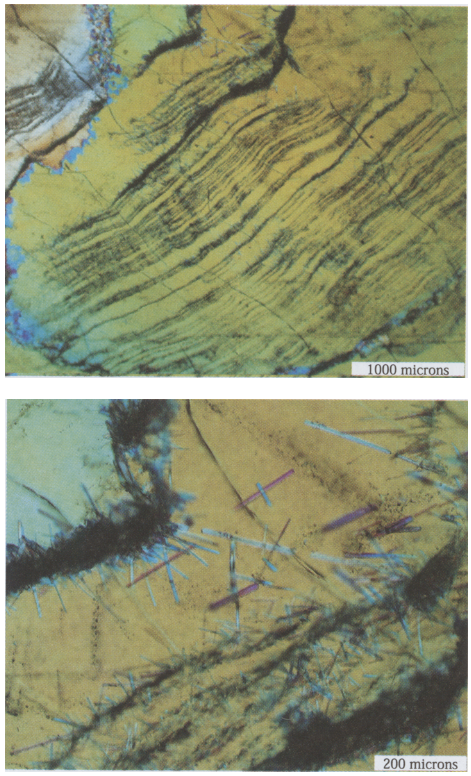

a) b)

**Fig. 2.** (**a**) Crack–seal sequence (crossed polars) of dark layers of tourmaline and light layers of quartz in gold-bearing quartz veins, Abitibi, Canada (sample S42abc). (**b**) Tourmaline fibres have nucleated from the crack wall-forming rosettes. This indicates that nucleation occurred far from equilibrium and that crystals grew in an open space.

## *Serpentine veins, San Andreas system, California*

Serpentine samples have been collected north of Santa Barbara (California), along the Santa Ynez fault, in the Blue Canyon. From late Jurassic to late Cenozoic times, this area has undergone subduction of the Pacific plate (Atwater 1989), resulted in an accretionary complex along the coast. In California, this so-called Franciscan subduction complex is a mélange of different sedimentary and ultramafic rocks, showing various degrees of deformation and metamorphism under HP-LT (e.g. Ernst 1971; Page 1981). Bodies of serpentinite are distributed throughout the mélange (Page 1972). They are derived from mantle peridotites that are partially to totally hydrated. Outside the highly deformed zones, massive serpentinites are preserved and show a network of hydrothermal veins, comparable to those described in oceanic ridge serpentinites (Dilek *et al.* 1997; Stamoudi 2002).

Extensional veins have a banded internal fabric (Fig. 3). They cross-cut at various orientations the serpentinized peridotite matrix that shows the typical mesh texture of replacement of olivine and pyroxene. They have been attributed to incremental stress release during progressive unroofing of serpentinites in the MARK area (Dilek *et al.* 1997). Like other veins of the same type, the banded veins considered here have irregular edges that are strictly parallel to each other. These criteria are similar to those invoked for incremental opening and filling by a crack–seal mechanism (Ramsay 1980). Minimum incremental opening is around 1 $\mu$m and the maximum observed is less than 5 $\mu$m.

Nanometer-size tubes of chrysotile (tubular serpentine mineral) have a preferred orientation perpendicular to the vein margins and fill each crack antitaxially. Thus, fibres do not directly track the displacement path, as observed in quartz veins by Cox (1987). However, the opening direction can be clearly followed thanks to a few inclusions of wall-rock and the undulose extinction linking edge irregularities across the vein. Bands are almost separated by a nanometric free space and tubes do not show any trace of deformation. In these veins, there is no evidence of cataclastic deformation; this could indicate that the mechanism of vein opening was a subcritical crack propagation process.

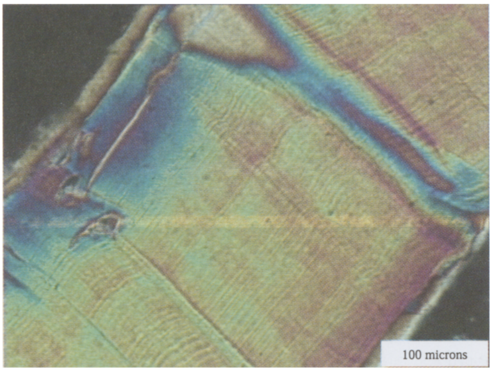


**Fig. 3.** Crack–seal sequence (crossed polars) in a serpentine vein, Santa Ynez fault, San Andreas system, California (sample SY3P). The individual cracks are filled with antiaxial serpentine fibres. The delicate geometry of the fibres has been conserved throughout time. The only disturbances are due to trapped impurities. This is indicative of a slow cracking mechanism, such as subcritical crack growth.

## *Calcite veins, Apennines, Italy*

Calcite crack–seal veins were collected in the Northern Apennines (NW Italy), a belt formed by stacked allochthonous units thrust toward the northeast from the Oligocene to the Recent (Elter 1973). In the northern part of the Bobbio window, where the sample comes from, several superficial units belonging to the Sub-Ligurian and Ligurian accretionary complexes have been thrust over lower Miocene turbidites of the Tuscan foredeep (Labaume & Rio 1994). The allochthon consists of mainly deep-sea marlstone, claystone and sandstone units, affected by low-angle faults. The tectonic pile was later folded antiformally, probably above a thrust.

Calcite veins are abundant in the marlstones of the allochthon, where they are commonly associated with scaly deformation marking the low-angle shear zones (Labaume *et al.* 1991). The most common veins are tabular bodies 1 to 5 cm in thickness and several metres to tens of metres in length. They consist of several superposed mm-thick calcite sheets with striated surfaces. Internal microstructures show that each calcite sheet is a shear vein. Calcite has crystallized in a large number of rhomb-shaped cavities, which are releasing oversteps between the two bounding shear surfaces (Fig. 4). The acute angle between the shear surfaces and the initial rupture, responsible for each overstep, gives an unambiguous indication of shear sense. This angle suggests a mode I rupture, that is, subparallel to the local direction of greatest principal stress. The direction of subsequent opening was

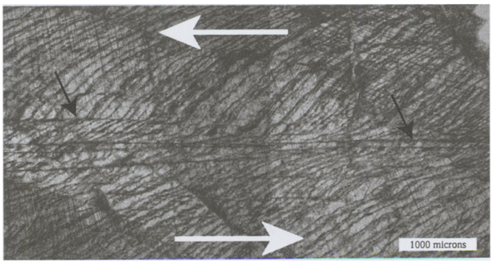


**Fig. 4.** Crack–seal sequence (ordinary light) in a calcite vein, Apennines, Italy (sample X45FXC). Calcite crystals appear in light colours whereas dark marlstone particles detached from walls of vein line the limit of each crack–seal surface. White arrows indicate direction and sense of shear; black arrows indicate shear surfaces.

controlled by movement along the shear surfaces. This is a similar geological setting to what Davison (1995) has described in limestones from Kilve, UK.

Releasing oversteps form sequences of many narrow calcite veinlets, separated by thin bands of encasing sediment (matrix bands) and bounded by closely spaced (<5 mm) shear surfaces. Individual veinlet width varies from 0.025 to 1 mm, the most common values being around 0.1 mm. For each veinlet, the shape-ratio (length of initial rupture to opening width) is usually well in excess of 10. Matrix bands are mostly extremely thin, relative to adjacent veins, and locally discontinuous. The veinlets formed sequentially, each releasing overstep opening only after the crystallization of calcite in the previously formed neighbouring overstep. The presence of the matrix bands shows that successive ruptures occurred preferentially in the sediment rather than at the calcite–sediment interface. This may be due to incomplete cementation of the very fine-grained sediment, allowing the pores to be invaded by calcite close to the veinlet walls. During the following rupture this thin band of sediment impregnated by calcite remained glued to the vein-fill, thus forming the matrix band that separates neighbouring veins. The crack–seal vein sequences are commonly offset a few tenths of millimetres by microtransform faults subparallel with the shear surfaces (Fig. 4). Some of these transform faults appear to have initiated at heterogeneities (e.g. fossil debris or a large siliciclastic grain), which locally hardened the sediment, thus deviating the ruptures.

## Statistical analysis of crack–seal pattern

Polished thin sections observed under an optical microscope with crossed polars were used to extract digital pictures with a high-resolution CCD camera. The position of each crack on a line was measured parallel to the direction of vein opening. The vein wall is set as the origin, and successive cracks are characterized by their distance from the origin. The distance between crack $n$ and crack $n+1$ is the aperture of crack $n$. This was calculated directly on the digitized images. The resolution of the measurement is around 0.5 micron (pixel size of the camera) for the highest optical magnification.

Using the crack position data and spatial derivative it was possible to construct cumulative displacement curves, distribution histograms, and crack thickness frequency plots. In addition, the signal was binarized by replacing the information on crack positions, pixel by pixel: the pixel is replaced by a ‘0’ if it does not contain a crack and by ‘1’ if it contains a crack boundary. This binarization process enables the relative spatial location of each crack to be reproduced. The binarized data set, determined directly from the previous one, is used to calculate Fourier transforms of the signal and therefore to study the spatial correlation properties of the pattern.

### *Crack thickness histograms: a characteristic length scale*

For each crack–seal vein, the position of each crack is plotted as a function of vein opening (Fig. 5, left). This plot shows how successive crack thicknesses stack spatially and characterizes the series of opening events. The cumulative opening of the vein is found to be almost a linear function of crack position. On average, the number of cracks on a segment parallel to the opening vector depends only on the length of the segment.

The derivative of this curve gives the thickness of each successive crack as a function of its position in the vein (Fig. 5, middle). The histograms of thicknesses (right column of Fig. 5) indicate that there is a characteristic length scale and a tail of thicker cracks. These thickness–frequency distributions are shown in the following to follow an exponential relationship.

### *Distribution function: exponential distribution of crack thicknesses*

The crack thickness data (Fig. 5, middle) are sorted according to decreasing thickness. We use the so-called rank-ordering technique (Zipf 1949), whereby variables are arranged in descending order $w_1 > w_2 > \cdots > w_n$ and crack thickness $w$ is plotted as a function of the

**Fig. 5.** Analysis of crack–seal data for six different crack–seal patterns (see Table 1). For each sample, the data analyses indicate similar results. Left column: cumulative displacement (i.e. distribution function) of the cracks, perpendicularly to the vein. Crack labelling starts near the vein wall (no. 1) and stops towards the centre of the vein (last crack–seal increment number). Middle column: thickness of cracks as a function of position in the series. This is the derivative of the curve in the left. Right column: histograms of crack thicknesses for the various samples. All distributions have tails for large thicknesses and a characteristic peak indicating a preferential crack thickness. The mean crack thickness is also shown.

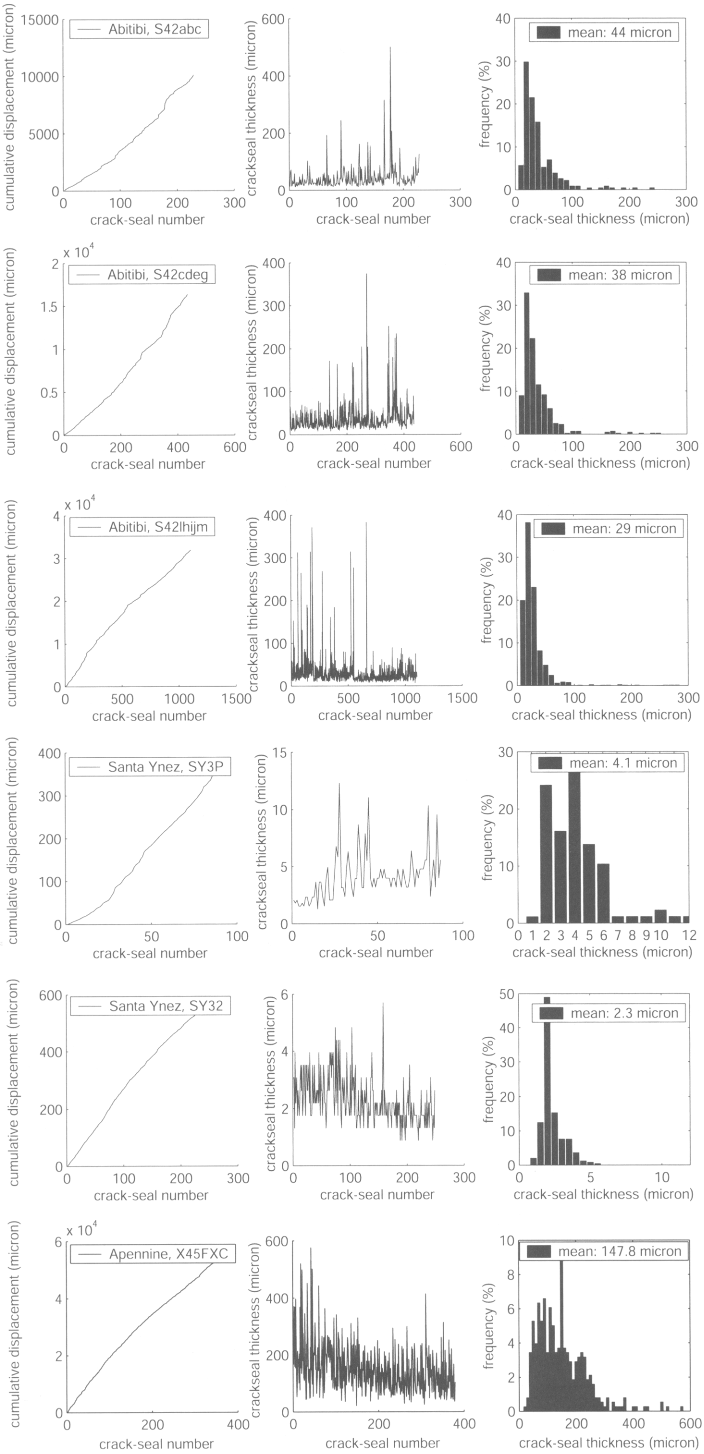
Abitibi, S42abc
mean: 44 micron
Abitibi, S42cdeg
mean: 38 micron
Abitibi, S42lhijm
mean: 29 micron
Santa Ynez, SY3P
mean: 4.1 micron
Santa Ynez, SY32
mean: 2.3 micron
Apennine, X45FXC
mean: 147.8 micron
cumulative displacement (micron)
crackseal thickness (micron)
frequency (%)
crack-seal number
crack-seal thickness (micron)
x 10^4

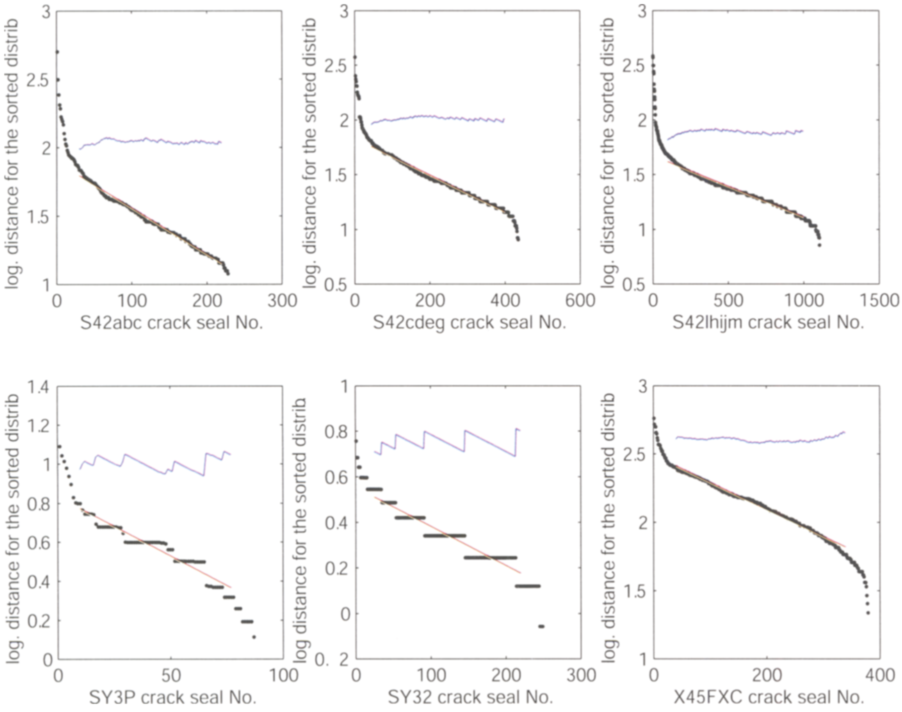


**Fig. 6.** Distribution of crack thicknesses. The data of the middle column in Figure 5 are sorted by decreasing thickness (rank-ordering technique). In a log-linear plot, the sorted data (black line) plot close to a straight line (red) over 80% of the signal (except for large and small cracks), indicating an exponential distribution. Residuals (blue line) have a mean value close to zero and no specific trend.

rank $n$. Represented in a log-linear diagram, the rank ordering plot is qualified by a straight line on more than 80% of each data set (Fig. 6).

This plot represents the distribution function of the cracks in a direction parallel to the opening vector and this describes the cumulative distribution of the probability density function. The distribution is mostly linear in a log-linear diagram, indicating that the data can be described by an exponential function (Otnes & Enochson 1978) where the number $n$ of cracks of thickness $w$ obeys the relationship

$$n(w) \propto \exp\left(-\frac{w}{w_0}\right) \quad (1)$$

The characteristic scale $w_0$ represents a physical length or arises through the dynamics of the fracturing process (Bonnet *et al.* 2001). Note that for the serpentine samples, the exponential distribution is not smooth, because the average crack aperture is close to the resolution of the optical measurement process.

For an exponential distribution, the mean and the standard deviation of the data set should be equal to $w_0$. Table 1 shows that for all crack–seal patterns, the mean crack thickness and the standard deviation are reasonably close. This measurement and the linear trends in Figure 6 indicate that the crack–seal data can be described by an exponential distribution, the deviation from an ideal distribution being small at small and large crack thicknesses. The large number of events (up to 1106 successive cracks for sample S42lhijm) ensures that the exponential distribution is representative.

### *Fourier analysis: absence of spatial correlation*

To study the spatial correlation of successive cracks, the Fourier transform of the binarized crack–seal patterns was calculated. In a log–log plot, the Fourier spectrum shows a flat linear relationship (Fig. 7). This indicates that the crack–seal data behave like a random series, having no preferential correlation in the signal: the variations of crack thickness are not correlated spatially between each other.

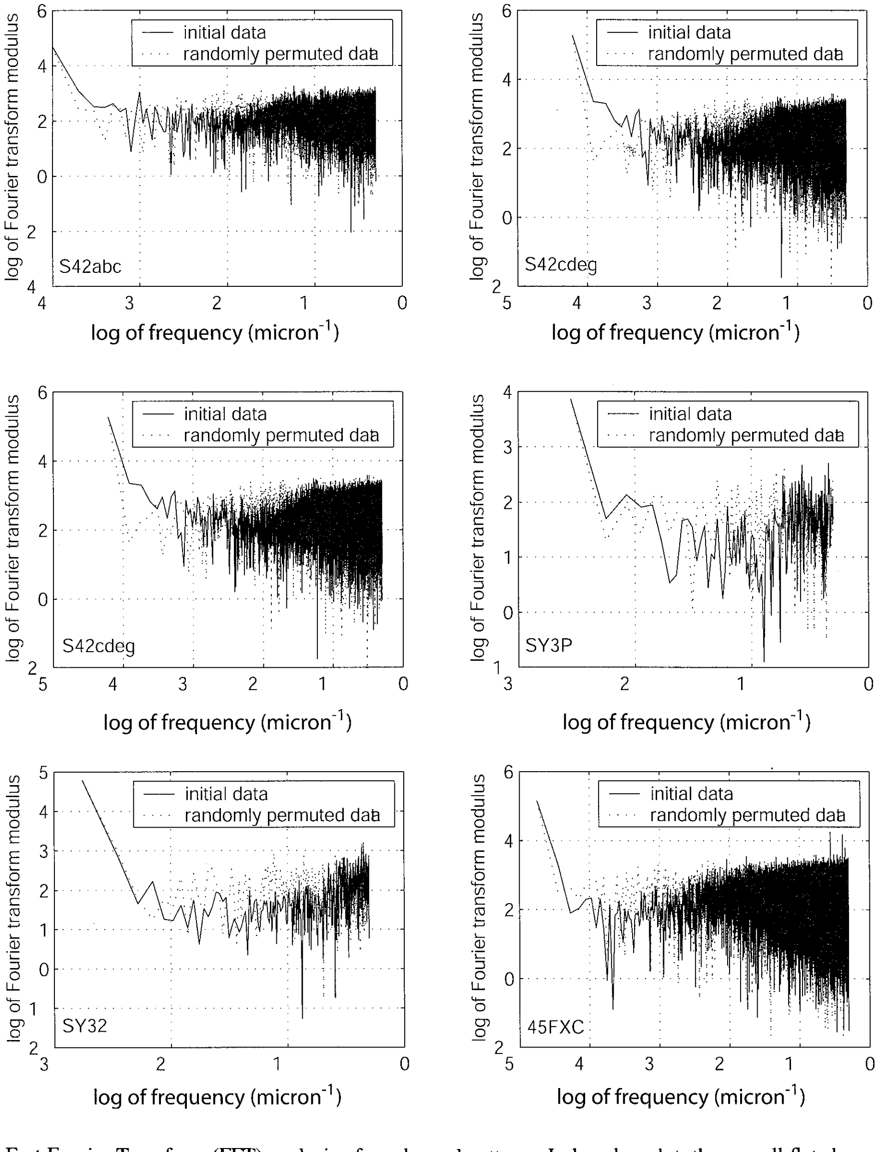


**Fig. 7.** Fast Fourier Transform (FFT) analysis of crack–seal patterns. In log–log plot, the overall flat shape of the Fourier spectrum indicates that noise dominates the data and that no specific organization can be detected. The raw data (full lines) and the randomly permutated data (dotted lines) show a similar horizontal linear trend.

This interpretation was confirmed by performing Fourier transforms on randomly permuted sets of data. For each crack–seal sequence, the positions of the cracks along the profile parallel to the vein opening direction were randomly permuted. This transformation gives series with the same mean and variance as the original ones and for which the initial order (spatial correlation), if any, is destroyed (dotted lines on Fig. 7). Performing Fourier transforms on these new sets does not change the flatness of the Fourier spectrum.

The question as to whether binarization of the original patterns taken with the camera could induce a bias on the high frequencies in the Fourier analysis needs to be addressed. To test this effect, Fourier transforms were also performed on the raw data, taken directly from the camera. Here again, the Fourier spectrum showed a flat linear relationship.

Another test, not shown here, is the autocorrelation function of the crack–seal sequence. For all samples, the autocorrelation function drops to zero immediately (as for randomly permutated data sets) thereby confirming that the crack–seal patterns are uncorrelated in space. Therefore, the successions of crack–seal thicknesses do not show any visible spatial organization. This is a memoryless process (the thickness of crack number $n$ does not depend on the thickness of crack $n-1$), which is also a property of exponential distributions.

## Discussion

To summarize the statistical analysis, cracks have an exponentially decaying thickness distribution (Fig. 5). The mean and standard deviation crack distribution values are close and the distribution is almost linear in a log-linear diagram (Fig. 6). Moreover the cracking events are not spatially correlated (Fig. 7). The crack-thickness distribution has all the properties of an exponential distribution.

The exponential probability density function has been widely used to accurately describe the failure times in various systems (Fisz 1963; Otnes & Enochson 1978). It characterizes systems containing a large number of elements (transistors, elastic fibres, and so on) which break with a constant failure rate probability. As an analogy to these systems, the exponential distribution of cracks indicates that they are characterized by a single failure rate, which can be controlled, for example, by the external loading conditions.

Geological systems such as mid-oceanic ridges (Cowie *et al.* 1993) also exhibit an exponential distribution. Based on numerical simulations on a spring network model, Spyropoulos *et al.* (2002) have concluded that exponential distributions of fractures in rocks are indicative of an increase in brittle strain in a regime dominated by the heterogeneity in the system. Moreover, Gupta & Scholz (2000) have observed a transition from a power-law to an exponential distribution of faults as brittle deformation increases in the Afar area.

The three types of crack–seal veins show the same trend of statistical properties, regardless of the geological context, the type of rock and the vein kinematics (extensional or shear vein). The linear trend in the cumulative displacement plot (Fig. 5, left) is interpreted as being the fact that the far-field boundary loading conditions and the physico-chemical parameters during the crack–seal deformation did not vary notably; see also Davison (1995) for similar data. There is neither acceleration nor slow-down in average vein growth rate. As a result, the variations observed in crack thickness should reflect disturbances around a steady-state fracturing process in a constant environment. This steady-state fracturing process is determined both by far-field stress conditions and by the local petrography and stress field in the wall-rock. For example, the grain size in the wall-rock could control the average crack thickness through nucleation processes or local variations in the wall-rock yield strength.

Petrographic evidence also confirms that the P-T conditions did not change during vein formation. Intergrowths of quartz and tourmaline form the crack–seal pattern in the Abitibi quartz veins (Fig. 2). These two crystals have grown from hydrothermal conditions and mineral paragenesis and the fluid inclusions trapped in the successive layers indicate that the thermodynamic conditions (lithostatic pressure, temperature) have not changed much during the whole vein opening history (Firdaous 1995; Robert *et al.* 1995). Such observations are similar for the three types of veins. The crack–seal sequence represents cycles of breakage events and periods of quiescence during which the filling minerals have grown from a fluid. During that time, stress and temperature were kept more or less constant. Consequently, crack–seal structures have recorded a sequence of events occurring in a rock domain with almost invariant geological conditions. In this respect, they have recorded small variations around a steady state. A crack–seal vein accumulates elastic strain due to tectonic loading until the stress on it reaches the yield strength. At this stage a new crack forms. The presence of a well-defined peak in the crack–seal thickness distribution indicates that the yield stress varies around a mean value. The uncorrelated distribution of crack–seals and the exponential distribution of crack thicknesses can be interpreted by two effects. On one side, they can reflect spatial heterogeneities in the rock as a crack opens. On the other side, they can reflect time-effective stress and/or fluid pressure variations at the vein boundary.

In the first assumption, the exponential distribution could be due to fluctuations in the crack length or in the local rock strength. The average crack length was measured in the field or directly on the samples (Table 1) and remains almost constant for all the cracks in each vein. In addition, each crack follows exactly the same parallel path as the previous one. Moreover there is no evidence that the crack thickness is related to the local mineralogy of the wall-rock.

For the Abitibi samples, the wall-rock contains centimetre-long quartz phenocrystals along which several tens of cracks have developed. Locally, these cracks also show an exponential distribution, even if there is no variation in the wall rock. Therefore there is no structural evidence in the sample that the heterogeneity content varies spatially and that there were local variations in the strength of the vein.

In the second assumption, the crack thickness varies, whereas all the textural or geometric parameters of the veins remain unchanged. As the crack lengths are almost constant, the crack thickness variations reflect disturbances in the crack thickness/crack length ratio. Rock mechanics indicate that this ratio is directly related to the state of stress around a fracture and/or at a fracture tip. Given that, after the cracking event, the crack remains open, several authors have proposed that high fluid pressures open the cracks (Sibson *et al.* 1988; Boullier & Robert 1992). For a pressurized, elastically opened crack, crack width is proportional to the driving pressure (Pollard & Segall 1987). With this assumption, the overpressure $\sigma$, necessary to open a crack of length $c$ with an aperture $w$ is

$$\sigma = \frac{wE}{4c} \qquad (2)$$

(Guéguen & Palciauskas 1994). This corresponds to the elastic stress released when a new crack has opened. Crack surface areas are similar for all the individual cracks; only the crack thickness varies. In this case, the thickness can be used to calculate typical stress variations that allowed crack opening assuming that the crack length is known. What crack–seal structures record in fact are variations in elastic stress release during the vein formation. The values for $c$ given in Table 1 represent a maximum length for the cracks as observed in the outcrops or directly on samples. Given these lengths and the typical elastic modulus of the wall-rocks, the variations in crack thickness indicate minimum effective driving pressure variations ranging from 10 to 50 bars. These variations are small compared to the main stresses. However, they are sufficient to explain the crack–seal patterns.

## Conclusions

Crack–seal veins, recording several hundred successive crack events, have been analysed. All data sets show similar statistical properties, irrespective of the various geological settings and vein kinematics: the exponential crack distributions have many similarities with a random data set that has a well-defined characteristic length. In this way, the distributions are different from other fracture patterns, which obey power-laws (as in earthquakes) or other types of correlations. Crack–seal structures provide a fossil record of non-correlated crack sequences that have a well-defined average characteristic size: they have recorded noisy stress release variations in the crust.

This project has been supported by the CNRS through an *Action Thématique Innovante.* We would like to thank C. Pequegnat and D. Tisserand for technical help. We thank S. Cox and P. Meakin for fruitful discussions and F. Robert for providing the Abitibi crack–seal samples. We acknowledge reviews by M. Jessell, X. Zhang and P. Cobbold.

## References

ATKINSON, B. K. 1984. Subcritical crack-propagation in geological materials. *Journal of Geophysical Research*, **89**, 4077–4114.

ATWATER, T. 1989. Plate tectonic history of the northeast Pacific and western North America. *In*: WINTERER, E. L., HUSSONG, D. M. & DECKER, R. W. (eds) *The Eastern Pacific Ocean and Hawaii. Geology of North America*, Geological Society of America, Boulder, CO, 21–71.

BEACH, A. 1977. Vein arrays, hydraulic fractures and pressure solution structures in a deformed flysch sequence, S.W. England. *Tectonophysics*, **40**, 201–225.

BEUTNER, E. C. & DIEGEL, F. A. 1985. Determination of fold kinematics from syntectonic fibers in pressure shadows, Martinsburg slate, New Jersey. *American Journal of Science*, **285**, 16–50.

BONNET, E., BOUR, O., ODLING, N. E., DAVY, P., MAIN, I., COWIE, P. & BERKOWITZ, B. 2001. Scaling of fracture systems in geological media. *Reviews of Geophysics*, **39**, 347–383.

BONS, P. & JESSELL, M. 1997. Experimental simulation of the formation of fibrous veins by localised dissolution–precipitation creep. *Mineralogical Magazine*, **61**, 53–63.

BONS, P. 2000. The formation of veins and their microstructures. *Journal of the Virtual Explorer*, **2**, 12.

BOULLIER, A. M. & ROBERT, F. 1992. Palaeoseismic events recorded in Archaean gold-quartz vein networks, Val d'Or, Abitibi, Quebec, Canada. *Journal of Structural Geology*, **14**, 161–179.

COWIE, P. C., SCHOLZ, C. H., EDWARDS, M. & MALINVERNO, A. 1993. Fault strain and seismic coupling on mid-oceanic ridges. *Journal of Geophysical Research*, **98**, 17 911–17 920.

COX, S. F. & ETHERIDGE, M. A. 1983. Crack-seal fibre growth mechanisms and their significance in the development of oriented layer silicate microstructures. *Tectonophysics*, **92**, 147–170.

COX, S. F. 1987. Antitaxial crack-seal vein microstructures and their relationship to displacement paths. *Journal of Structural Geology*, **9**, 779–787.

COX, S. F. 1991. Geometry and internal structures of mesothermal vein systems: implications for hydrodynamics and ore genesis during deformation. *In*: *Structural Geology in Mining and Exploration*. University of Western Australia, *Extended Abstracts*, **25**, 47–53.

COX, S. F. 1995. Faulting processes at high fluid pressures: an example of fault valve behavior from the Wattle Gully Fault, Victoria, Australia. *Journal of Geophysical Research*, **100**, 12 841–12 859.

DAVISON, I. 1995. Fault slip evolution determined from crack-seal veins in pull-apart and their implications for general slip models. *Journal of Structural Geology*, **7**, 1025–1034.

DILEK, Y., COULTON, A. & HURST, S. D. 1997. Serpentinization and hydrothermal veining in peridotites at site 920 in the Mark area. *In*: KARSON, J. A., CANNAT, M., MILLER, D. J. & ELTHON, D. (eds) *Proceedings of the Ocean Drilling Program, Scientific Results*, **153**, 35–59.

ELLIS, M. 1986. The determination of progressive deformation histories from antitaxial syntectonic crystal fibers. *Journal of Structural Geology*, **8**, 701–709.

ELTER, P. 1973. Lineamenti tettonici ed evolutivi dell Appennino. *Acad. Naz. Lincei, Roma*, **183**, 97–109.

ERNST, W. G. 1971. Do mineral parageneses reflect unusually high pressure conditions of Franciscan metamorphism? *American Journal of Science*, **271**, 81–108.

FIRDAOUS, K. 1995. *Etude des fluides dans une zone sismogénique fossile: les gisements aurifères mésothermaux archéens de Val d'or, Abitibi, Québec*. University Thesis, Institut National Polytechnique de Lorraine.

FISHER, D. M. & BRANTLEY, S. L. 1992. Models of quartz overgrowth and vein formation: deformation and episodic fluid flow in an ancient subduction zone. *Journal of Geophysical Research*, **97**, 20 043–20 061.

FISHER, D. M., BRANTLEY, S. L., EVERETT, M. & DZVONIK, J. 1995. Cyclic fluid flow through a regionally extensive fracture network within the Kodiak accretionary prism. *Journal of Geophysical Research*, **100**, 12 881–12 894.

FISZ, M. 1963. *Probability Theory and Mathematical Statistics*. Wiley Publications in Statistics, Wiley, New York.

GAVIGLIO, P. 1986. Crack-seal mechanism in a limestone: a factor of deformation in strike-slip faulting. *Tectonophysics*, **131**, 247–255.

GUÉGUEN, Y. & PALCIAUSKAS, V. 1994. *Introduction to the Physics of Rocks*. Princeton University Press, Princeton, NJ.

GUPTA, A. & SCHOLZ, C.H. 2000. Brittle strain regime transition in the Afar depression: implications for fault growth and sea-floor spreading. *Geology*, **28**, 1087–1090.

HENDERSON, J. R., HENDERSON, M. N. & WRIGHT, T. O. 1990. Water-sill hypothesis for the origin of certain veins in the Meguma Group, Nova Scotia, Canada. *Geology*, **18**, 654–657.

HILGERS, C. 2000. *Vein growth in fractures: experimental, numerical and real rock studies*. Unpublished PhD dissertation thesis, University of Aachen, Germany.

LABAUME, P., BERTY, C. & LAURENT, P. 1991. Syndiagenetic evolution of shear structures in superficial nappes: an example from the Northern Apennines, NW Italy. *Journal of Structural Geology*, **13**, 385–398.

LABAUME, P. & RIO, D. 1994. Relationships between the subLigurian allochthon and the Tuscan foredeep turbidites in the Bobbio window (NW Apennines). *Memorie della Società Geologica Italiana*, **48**, 309–315.

OTNES, R. K. & ENOCHSON, L. 1978. *Applied Time Series Analysis*. Wiley, New York.

PAGE, B. M. 1972. Oceanic crust and mantle fragment in subduction complex near San Luis Obispo, California. *Geological Society of America Bulletin*, **83**, 957–972.

PAGE, B. M. 1981. The Southern Coast Range. *In*: ERNST, G. W. (ed) *The Geotectonic Development of California*. Prentice-Hall, Englewood Cliffs, New Jersey, 330–417.

PASSCHIER, C. & TROUW, R. 1995. *Microtectonics*. Springer, Berlin.

PETIT, J.-P., WIBBERLEY, C. A. J. & RUIZ, G. 1999. Crack-seal, slip: a new fault valve mechanism? *Journal of Structural Geology*, **21**, 1199–1207.

POLLARD, D. D. & SEGALL, P. 1987. Theoretical displacement and stresses near fractures in rock with applications to faults, joints, veins, dykes and solution surfaces. *In*: ATKINSON B. K. (ed) *Fracture Mechanics of Rock*. Academic Press, London, 277–350.

RAMSAY, J. G. 1980. The crack-seal mechanism of rock deformation. *Nature*, **284**, 135–139.

RAMSAY, J. G. & HUBER, M. I. 1983. *The Techniques of Modern Structural Geology. Volume 2: Folds and Fractures*. Academic Press, London.

ROBERT, F. 1990. Structural setting and control of gold-quartz veins of the Val d'Or area, southeastern Abitibi Subprovince. *In*: HO, S. E., ROBERT, F. & GROVES, D. I. (eds) *Gold and Base Metal Mineralization in the Abitibi Subprovince, Canada, with Emphasis on the Quebec Segment*. University of Western Australia Publication, **24**, 164–209.

ROBERT, F. & BOULLIER, A. M. 1994. Mesothermal gold-quartz veins and earthquakes. *In*: HICKMAN, S. H., SIBSON, R. H. & BRUHN, R. L. (eds) *The Mechanical Involvement of Fluids in Faulting*. U.S. Geological Survey, Open-file report 94-228, 18–30.

ROBERT, F., BOULLIER, A. M. & FIRDAOUS, K. 1995. Gold-quartz veins in metamorphic terranes and their bearing on the role of fluids in faulting. *Journal of Geophysical Research*, **100**, 12 861–12 879.

ROBERT, F. & BROWN, A. C. 1986. Archean gold-bearing quartz veins at the Sigma Mine, Abitibi greenstone belt, Quebec. Part I: Geologic relations and formation of the vein systems. *Economic Geology*, **81**, 578–592.

SIBSON, R. H., ROBERT, F. & POULSEN, K. H. 1988. High angle reverse faults, fluid-pressure cycling and mesothermal gold quartz deposits. *Geology*, **16**, 551–555.

SPYROPOLOUS, C., SCHOLZ, C. H. & SHAW, B. E. 2002. Transition regimes for growing crack populations. *Physical Review E*, **65**, 056105-1–056105-10.

STAMOUDI, C. 2002. *Processus de serpentinisation des péridotites de Hess-Deep et de la zone de MARK: Approches chimiques et minéralogiques.* PhD thesis, University Paris VI, France.

TABER, S. 1916. The growth of crystals under external pressure. *American Journal of Science*, **XLI** (4th series, No. 246), 532–556.

TABER, S. 1918. The origin of veinlets in the Silurian and Devonian strata of central New York. *Journal of Geology*, **6**, 56–73.

TORIUMI, M. & HARA, E. 1995. Crack geometries and deformation by the crack-seal mechanism in the Sambagawa metamorphic belt. *Tectonophysics*, **245**, 249–261.

URAI, J. L., WILLIAMS, P. F. & van ROERMUND, H. L. M. 1991. Kinematics of crystal growth in syntectonic fibrous veins. *Journal of Structural Geology*, **13**, 823–836.

VAN DER PLUIJM, B. A. 1984. An unusual 'crack-seal' vein geometry. *Journal of Structural Geology*, **6**, 593–597.

WILLIAMS, P. F. & URAI, J. L. 1989. Curved vein fibres: an alternative explanation. *Tectonophysics*, **158**, 311–333.

WILTSCHKO, D. V. & MORSE, J. W. 2001. Crystallization pressure versus 'crack seal' as the mechanism for banded veins. *Geology*, **29**, 79–82.

XU, G. 1997. Fluid inclusions in crack-seal veins at Dugald River, Mount Isa Inlier: implications for paleostress states and deformation conditions during orogenesis. *Journal of Structural Geology*, **19**, 1359–1368.

ZIPF, G. K. 1949. *Human Behavior and the Principle of Least-Effort.* Addison-Wesley, Cambridge.